WPJET3-PR(18) 19298

B Obryk et al.

TLD calibration for neutron fluence measurements at JET fusion facility

Preprint of Paper to be submitted for publication in
Nuclear Instruments and Methods in Physics Research
Section A

This work has been carried out within the framework of the EUROfusion Consortium and has received funding from the Euratom research and training programme 2014-2018 under grant agreement No 633053. The views and opinions expressed herein do not necessarily reflect those of the European Commission.

TLD calibration for neutron fluence measurements at JET fusion facility

B. Obryk[a,1], R. Villari[b], P. Batistoni[b], A. Colangeli[b], P. De Felice[b], N. Fonnesu[b], M. Kłosowski[a], S. Loreti[b], K. Malik[a], J. Nash[c], M. Pillon[b], M. Pimpinella[b], L. Quintieri[b], and JET Contributors[2]

EUROfusion Consortium, JET, Culham Science Centre, Abingdon, OX14 3DB, UK
[a]Institute of Nuclear Physics Polish Academy of Sciences (IFJ PAN), ul. Radzikowskiego 152, 31-342 Kraków, Poland
[b]ENEA, Department of Fusion and Technology for Nuclear Safety and Security, I-00044 Frascati (Rome) & I-00123 Santa Maria di Galeria (Rome), Italy
[c]CCFE Culham Science Centre, Abingdon, Oxon, OX14 3DB, UK

Abstract

Measurements of neutron streaming through penetrations in the biological shield are being carried out at JET fusion device using thermoluminescence (TL) detectors with the objective to validate in a real fusion environment the neutronics codes and nuclear data applied in ITER nuclear analyses. The response of TLDs due to the neutron component of the radiation field is related to the neutron fluence in a well-defined neutron energy spectrum. Therefore, there was a need of TLDs' calibration in real fusion radiation fields which will allow for more correct calculation of neutron fluence from TL measurements at JET. In order to perform this task MCP-N and MCP-7 TLDs produced at the IFJ PAN in Kraków were calibrated in the ENEA facilities of Frascati and Casaccia laboratories. Analyses of the results have been performed and determination of new calibration factors are proposed. The detection system based on TLDs developed and calibrated for JET experiments can be applied more generally in fusion neutron fields and, for example, in ITER to monitor the neutron fluence outside the biological shield.

Keywords: thermoluminescence; lithium fluoride; neutron fluence, fusion, neutron generator, JET

1. Introduction

Neutronics experiments are being carried out at JET which aims at validating in a real fusion environment the neutronics codes and nuclear data applied in ITER nuclear analyses. Among other experiments, the measurements of the neutron fluence through the penetrations of JET Torus Hall aim at assessing the capability of numerical tools to correctly predict the radiation transport along the long paths and the complex geometries characterizing the ITER biological shield. Neutron streaming measurements started at JET in 2012 DD campaign in preparation of experiments to be carried out with full DT operation, and the first results were reported in 2013 and 2014 while further measurements took place during 2015-2016 DD/DT campaigns [1-6]. The experimental positions of the last neutron streaming experiment at JET are shown in figure 1 [5].Very sensitive lithium fluoride based, doped with magnesium, copper and phosphorus (LiF:Mg,Cu,P) thermoluminescence detectors (TLDs) [7-8] which are able to measure radiation doses from fractions of μGy up to about MGy [9-11] were used for absorbed dose and neutron fluence measurements. The use of LiF TLDs, enriched to different levels in ^{6}LiF/^{7}LiF allowed distinguishing between neutron and non-neutron components of the radiation field [12-14]. The response of TLDs due to the neutron component is related to the neutron fluence in a well-defined neutron energy spectrum. In particular, the part of TLDs response due to neutron component of the radiation field

[1] Corresponding author: e-mail: barbara.obryk@ifj.edu.pl; tel.: +48-12-6628280; fax: +48-12-6628066
[2] See the author list of X. Litaudon et al. 2017 Nucl. Fusion 57 102001

can be related to the local neutron fluence taking into account LiF detectors' calibration at the PTB Thermal Neutron Reference Field at GeNF [15] performed in 2006 by Burgkhardt et al. [16]. The TLDs were calibrated at GeNF in a thermal neutron spectrum. In the case of JET measurements, although the neutron spectrum is not thermal in the Torus Hall, the use of large cylindrical PE moderators (diameter 25.5 cm, height 21-25 cm) ensures that the enclosed TLDs "see" a thermal neutron field, with this assumption the 'Burgkhardt' calibration factors [16] can be applied. Actually, close to the tokamak, the neutron field inside the PE cylinder is not fully thermalized and the detectors are exposed to a significant fast neutrons component. The TLDs calibration factors from Burgkhardt et al. [16] are therefore not correct in these positions.

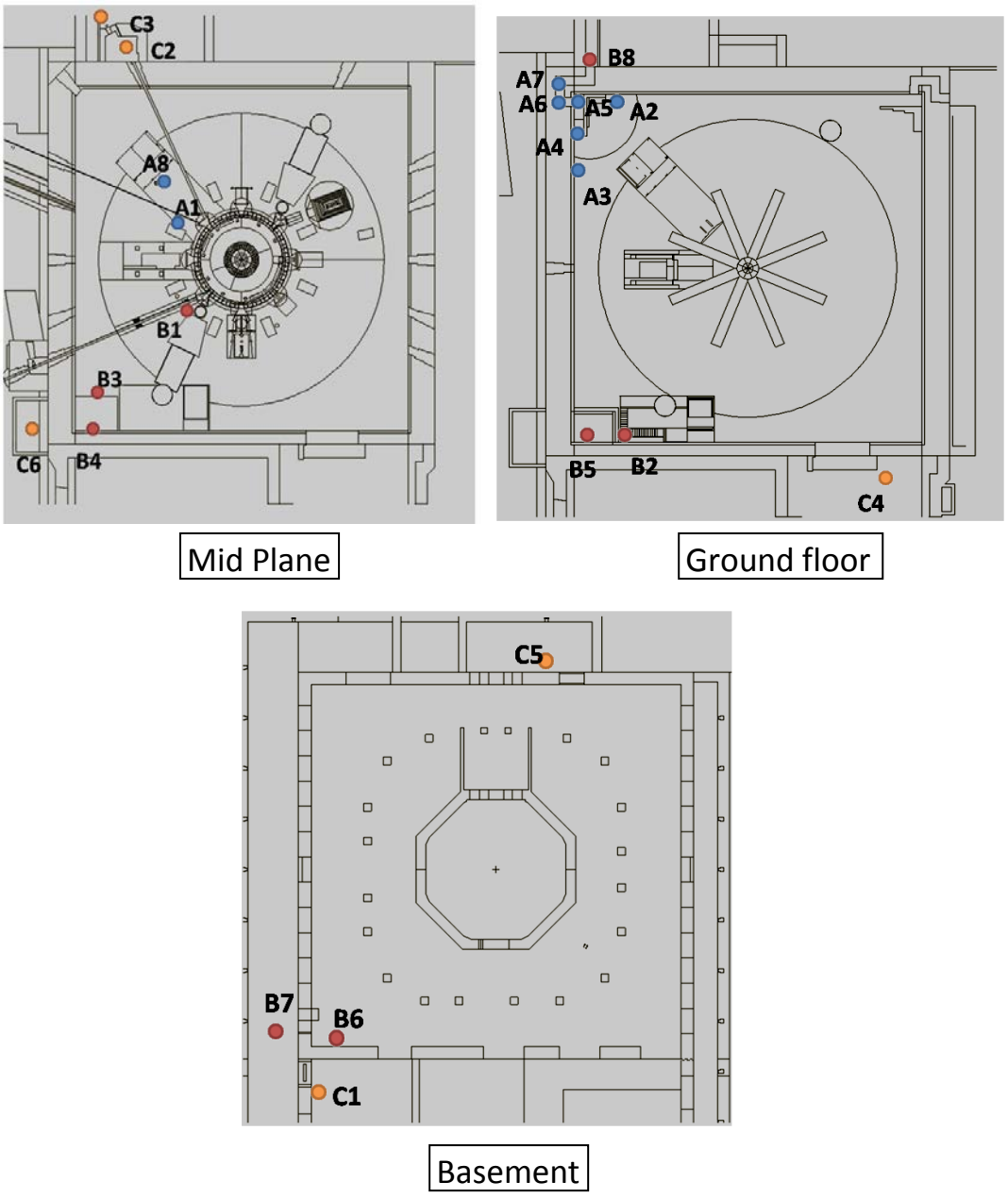

Figure 1. Overview of positions of the detectors for the 2015 DD JET neutron streaming experiments [5]. Note that the detectors are at different levels.

Because of this, there was a need of more accurate TLDs calibration in real fusion radiation fields which will allow for more correct calculation of neutron fluence from TL measurements at JET. In order

to perform this task, MCP-N (^{nat}LiF:Mg,Cu,P) and MCP-7 (^{7}LiF:Mg,Cu,P) TLDs produced by the IFJ PAN were calibrated in the ENEA facilities of Frascati and Casaccia laboratories in November and December 2016. TLDs in bare rectangular holders, and TLDs in rectangular and cylindrical holders inside moderators (same assembly as JET experiment) were irradiated under DD (2.5 MeV) and DT (14 MeV) neutrons at the Frascati Neutron Generator (FNG) [17]. Bare irradiations were performed at 6 positions from 5.5 to 88.5 cm distance from FNG target. Positions and irradiation times were selected on the basis of pre-analysis carried-out with MCNP5 [18] to cover a range of neutron fluence of 2 orders of magnitude relevant for JET experiment. Bare irradiations lasted about 3 hours (under DD) and 7 minutes (under DT) with a neutron yield of ~2.23×10^{12} n and the fluence at detectors positions in the range 3×10^{7} -10^{10} n/cm^2. Further separate irradiations (5 under DD and 5 under DT) were performed inside polyethylene moderators (cylindrical & rectangular holders in the plug assembly used during past JET streaming experiments) at the same positions as bare (except the first one). The irradiations lasted between 55 min and 106 min under DD and 3-6 min under DT, to provide to TLDs, inside the moderators, the same level of fluence as the bare configuration. This allows one to evaluate the moderator's body influence on the enhancement of thermal neutron signal registered by TLDs. The results will allow one to increase the accuracy of neutron fluence calculation at JET by replacing the calibration coefficients from Burgkhardt et al. [16] designated in the field of thermal neutrons with new coefficients which take into account the characteristics of neutron fields at fusion facilities. Accurate MCNP simulations of the real experimental set-up were performed to calculate the neutron spectra at the TLDs positions under DD and DT neutrons, for the assessment of the new calibration factors.

Irradiations of proper bare samples in cylindrical holders under Co-60 gamma source and in thermal neutron facility were carried-out at INMRI (Istituto Nazionale di Metrologia delle Radiazioni Ionizzanti) laboratories in ENEA Casaccia. The TLDs were exposed at Co-60 source to air kerma of 100 mGy, 1 Gy and 5 Gy. Five samples in cylindrical holders (same as those used in JET assembly) were exposed to thermal neutrons from 30 minutes to 48 hours (neutron fluence in the range 2×10^{7} - 2×10^{9} n/cm^2). TLDs were sent back to IFJ for read-out. Analyses of the results have been performed and determination of new calibration factors have been proposed.

2. Materials and methods

2.1 Preparation of the samples

2.1.1. LiF:Mg,Cu,P production procedure

All detectors' batches have been produced at the IFJ in Kraków using sintering method. For producing the MCP-N, first undoped lithium fluoride was synthesized in chemical processes between LiCl (AlfaAesar 99% reagent grade) and HF >48% (Sigma-Aldrich, puriss p. a.). The obtained LiF powder was thoroughly mixed with activators: $MgCl_2$ solution (obtained from magnesium oxide POCH S.A. pure p.a. with fuming hydrochloric acid for trace analysis by Sigma-Aldrich), $CuCl_2$ solution (obtained from cooper oxide POCH S.A. pure p.a. with fuming hydrochloric acid for trace analysis by Sigma-Aldrich) and H_3PO_4 (POCH S.A> pure p.a.). After drying, the mixture was then melted in a platinum crucible at 1070^{o}C under inert gas atmosphere. After a period of 70 minutes in the molten stage, the material in the crucible was quenched to 550^{o}C and then cooled rapidly to room temperature. After cooling, the material was grounded into small grains and sieved. For production of the detectors the grains from 63 µm up to 212 µm were used. In one batch near 20 g of powdered phosphor was obtained. Each production batch had the TL properties checked out. If the TL parameters (such as sensitivity level and shape of glow-curve) were correct, the batches were blended homogeneously.

For producing the MCP-7, the starting substance was lithium hydroxide monohydrate (99.96% ^{7}Li). In first step the lithium chloride was obtained (with reaction $^{7}LiOH*H_2O + HCl \rightarrow {}^{7}LiCl + 2*H_2O$), then the following steps of MCP-7 productions were the same as for MCP-N.

The homogeneously blended grain powders of each type were pressed mechanically into pellets of 4.5 mm diameter and 0.9 mm thickness. The last stage was the sintering of pellets at a temperature between 600-700^{o}C in gas atmosphere and platinum containers for a certain period of time, during which the LiF:Mg,Cu,P phosphor gains higher sensitivity. The pellets were then visually controlled. Cracked, deformed and smutted pellets were removed from the rest. The good quality pellets had TL properties controlled again. In this way batches of MCP-N and MCP-7 detectors have been produced and checked out. 400 pcs of MCP-N and 400 pcs of MCP-7 detectors were chosen for further preparation. All detectors were polished on both sides and labelled with numbers with a pencil.

2.1.2. Dosimeters' preparation for measurements.

In order to prepare the TL detectors for measurement the standard pre-irradiation annealing cycle was applied (two-phase heat treatment): 260°C for 10 minutes followed by 240°C for 10 minutes. The individual response factors of the detectors were also measured. During this process, all detectors were irradiated with the same dose of 1 mGy and readout using automatic TL reader. Then the individual response factors (IRF) have been derived in relation to the mean value of TL signal for all detectors of the same type. Finally, all detectors have undergone pre-irradiation annealing procedure next time in order to prepare them for measurement campaign.

Detectors' boxes have been filled in with detectors. For all irradiations the same boxes were used as during the measurements at JET [1-2]. For six 'bare' DD and six 'bare' DT exposures at FNG rectangular boxes were used, each box filled with 5 pcs of MCP-N and 5pcs of MCP-7 detectors. For DD and DT exposures in moderators the standard configuration used at JET has been used [1-2], see figure 2. For each of five DD and five DT exposures in moderators' circular and rectangular boxes with detectors have been prepared (figure 3). Each box contained 5 pcs of MCP-N and 5 pcs of MCP-7 detectors.

For thermal neutron exposures 5 circular boxes with 5 pcs of MCP-N and 5 pcs of MCP-7 detectors each have been prepared. For Co-60 gamma exposures 3 circular boxes with 5 pcs of MCP-N and 5 pcs of MCP-7 detectors each have been prepared. Also dosemeters to measure the background and transport dose have been prepared for each experiment. Each of them contained 5 pcs of MCP-N and 5 pcs of MCP-7 detectors and they were transported and kept together with experimental dosemeters. All dosemeters have been transported to Frascati on 20th November 2016. Some TLDs from each type were packed in 10 cm diameter polymethacrylate (PMMA) boxes and kept in low dose lead container/house at IFJ TLD laboratory for calibration purposes and background evaluation for calibration (so called calibration TLDs).

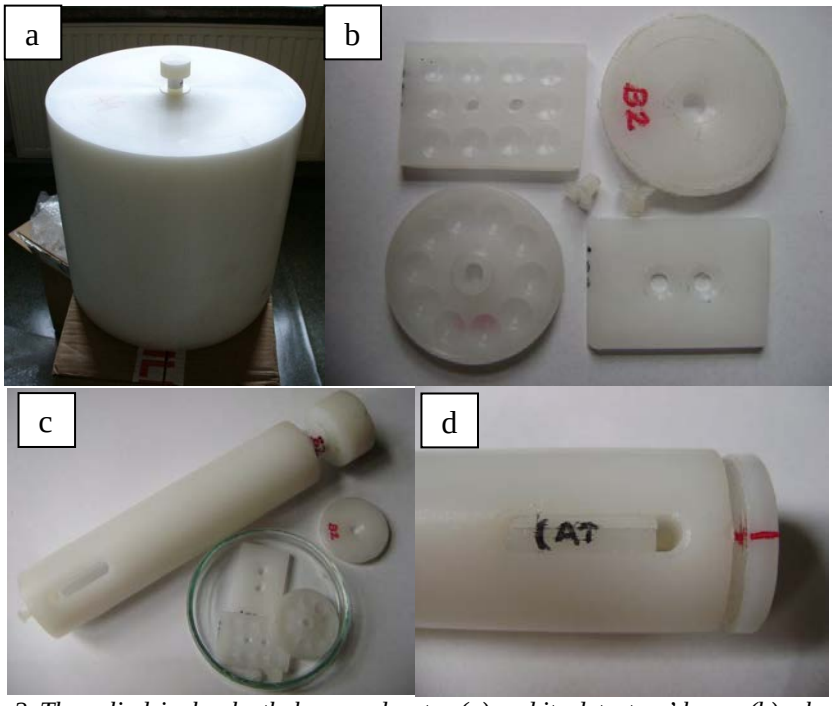

Figure 2. The cylindrical polyethylene moderator (a) and its detectors' boxes (b), plug and detectors' boxes (c), plug with detectors' boxes mounted (d).

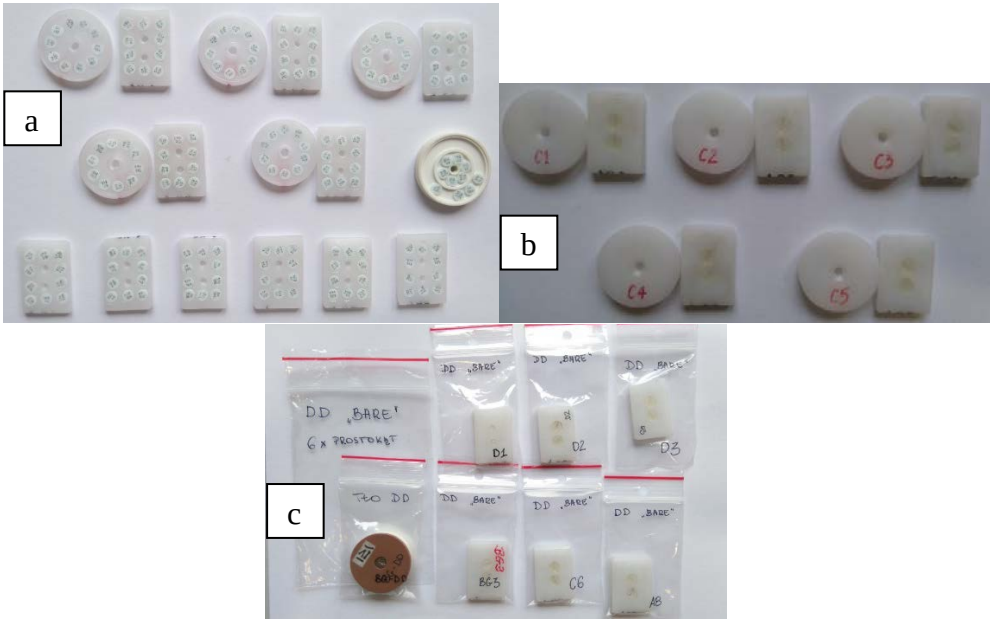

Figure 3. Detectors' boxes for DD exposures: a) filled in with detectors, b) prepared for moderators, c) prepared for bare exposures and packed for transport.

2.2. Irradiations at the Frascati Neutron Generator (FNG)

Irradiations of TLDs samples have been performed in bare configuration (figure 4) and inside the moderators (figure 5) under 2.5 MeV (DD) and 14 MeV (DT) neutrons at the Frascati Neutron Generator (FNG) [17]. The layout of the irradiation and positions have been defined on the basis of pre-analysis performed with MCNP5 to cover a range of fluence of more than 2 orders of magnitude and greater than $2x10^7$ n cm^{-2}, relevant for JET streaming experiment.

Figure 4. Picture of bare irradiation at FNG.

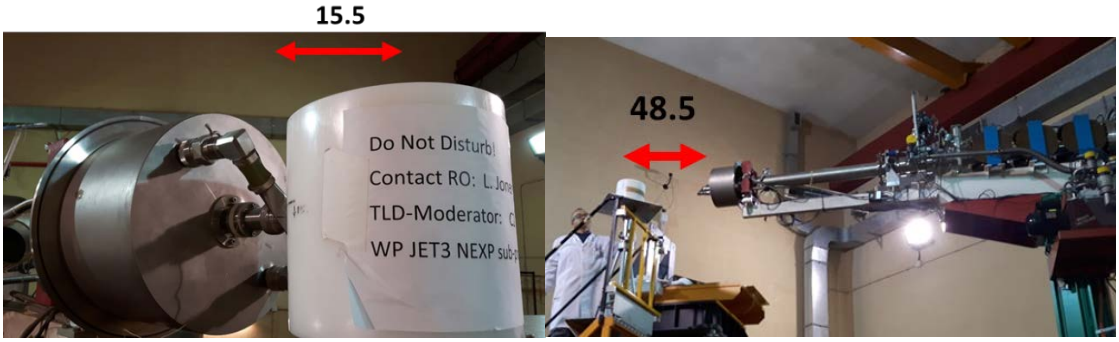

Figure 5. Pictures of the experimental assembly during irradiation in polyethylene moderator at FNG (two positions are shown).

2.2.1. Simulations with MCNP5

Monte-Carlo calculations were performed with MCNP5 code, and using the reference FNG MCNP model and source subroutine. In a first stage a pre-analysis was performed in order to define the experimental layout for the calibration under DD and DT neutrons. The MCNP geometrical model includes TLDs inside proper holders and PVC support rail in bare irradiation and inside PE-cylinder. The MCNP models are shown in figure 6. Six positions, for "bare" irradiation were selected: from 5.5 cm to 88.5 cm. For configuration inside moderator, five separate calculations, at the same distances as bare were performed from 15.5 cm to 88.5 cm. Simulations were carried-out in DD, 2.5 MeV neutrons, and in DT, 14 MeV neutrons.

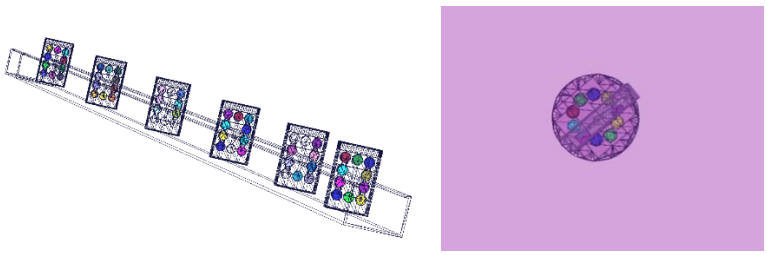

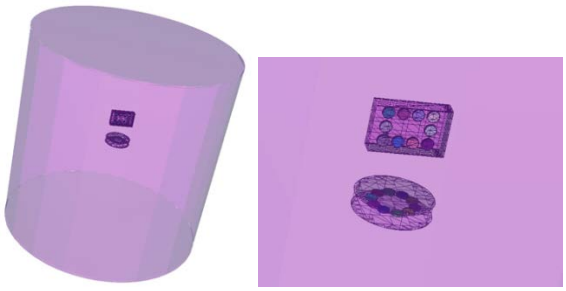

Figure 6. MCNP 3D model of: bare configuration (top left), top view of holders inside PE-cylinder (top right), cylinder + holders (bottom left) and front view of holders and TLDs (bottom right).

A. Simulations of DD&DT irradiations in bare holders

The total neutron and photon fluxes for DD (2.5 MeV) "bare" configuration have been calculated and are shown in figure 7. The total average flux over all MCP-7 is the same to that of MCP-N with a negligible variation. The gamma flux produced by interactions of neutrons with FNG target and surrounding components is lower than the neutron flux.

Figure 8 shows the average absorbed dose and air kerma in MCP-N and MCP-7 calculated for neutrons and gammas. The air kerma values due to neutrons are two orders of magnitude higher than those due to gammas. The air kerma shows negligible variations between MCP-N and MCP-7, whereas the absorbed dose due to neutrons is sensitive to Li-6 contents and the neutron dose in MCP-N is higher than in MCP-7.

The same simulations were done for DT (14 MeV) "bare" irradiations. Neutron and gamma fluxes are shown in figure 9. The secondary gamma flux is lower than the neutron flux by a factor 5 near the target and by a factor 1.6 at 88.5 cm. There aren't significant differences between MCP-7 and MCP-N in this case as well as in DD. Average absorbed dose and air kerma in MCP-N and MCP-7 for neutrons and gammas are in figure 10. It can be noted that the dose and air kerma are higher in DT than DD by a factor from 2 to 5, depending on the particle and position.

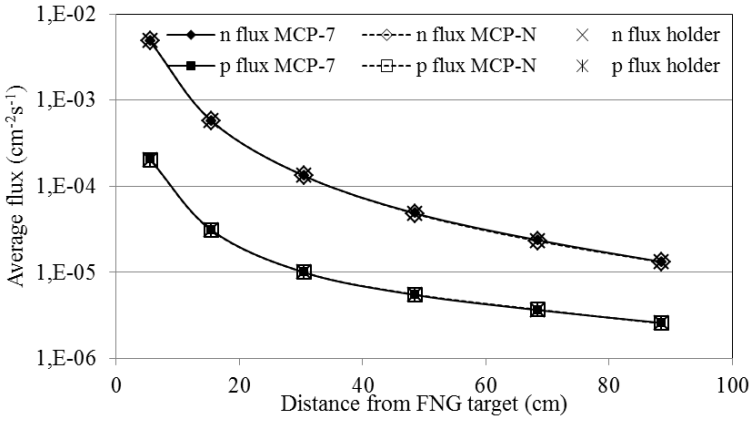

Figure 7. Neutron and photons fluxes per one source neutron vs. distance from FNG target in DD "bare" configuration.

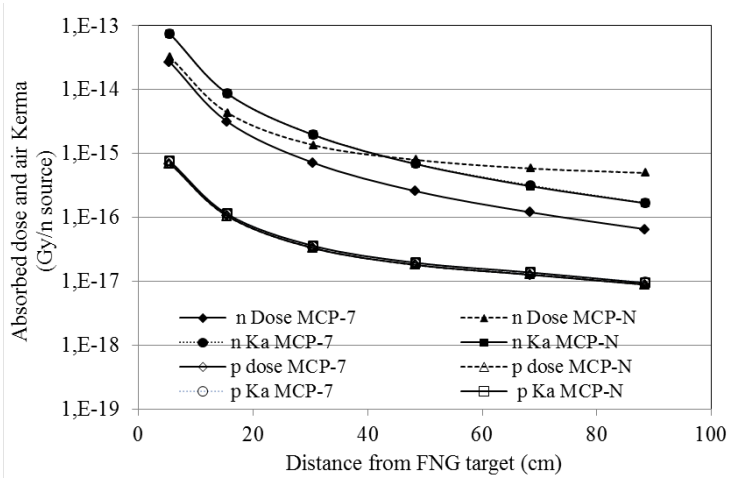

Figure 8. Neutron (n) and gamma (p) average absorbed dose per source neutron in TLD and air kerma (Gy/n source) for MCP-7 and MCP-N for DD "bare" configuration.

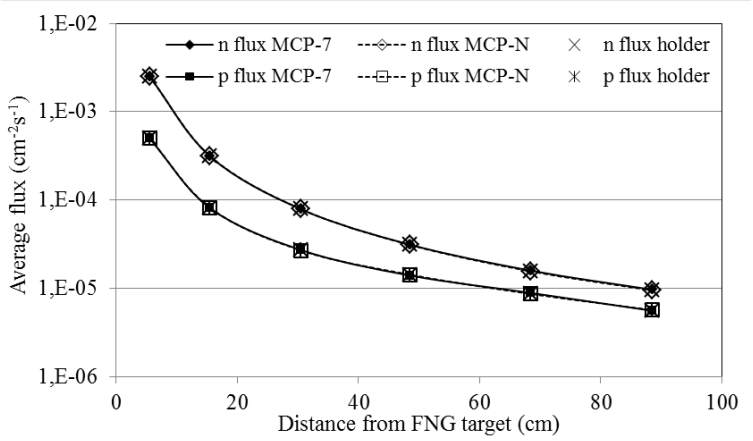

Figure 9. Average Neutron (n) and gamma (p) fluxes per source neutron in MCP-7 and MCP-N and overall TLDs under DT irradiation in "bare" configuration.

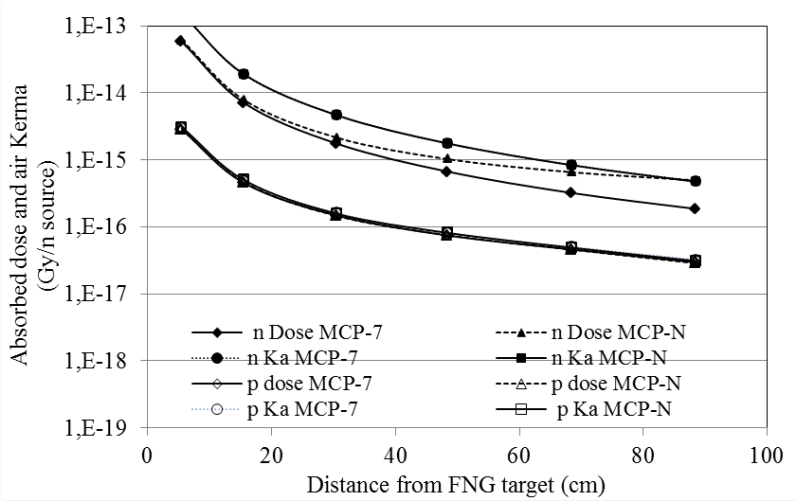

Figure 10. Neutron (n) and gamma (p) average absorbed dose per source neutron in TLD and air Kerma (Gy/ n source) for MCP-7 and MCP-N for DT "bare" configuration.

.

B. Simulations of DD&DT irradiations inside the PE moderators

Simulations were performed in polyethylene moderator at five radial distances from FNG target for DD and DT irradiation. Figure 11 shows the MCNP models of circular and rectangular holder inside PE moderator. The neutron and gamma flux results under DD are shown in figure 12 for rectangular holders (the same values are obtained for circular holders). The neutron flux inside MCP-7 is about 30% higher than in MCP-N. The gamma flux is lower than the neutron flux, on average, by a factor 3 in the first position and 2 in the last one.

The neutron fluxes distributions vary inside the cylindrical holders depending on TLD type and positions are shown in figure 13. The neutron flux inside the same types of TLDs inside circular holders is symmetric with respect to the Y-axis. MCNP results show these particular symmetries in the following pairs of TLDs: 8003 – 8004 (MCP-7), 8005 – 8013 (MCP-N), 8006 – 8012 (7), 8007 – 8011 (N). Total neutron and gamma fluxes are slightly lower in DT with respect to DD (figure 14).

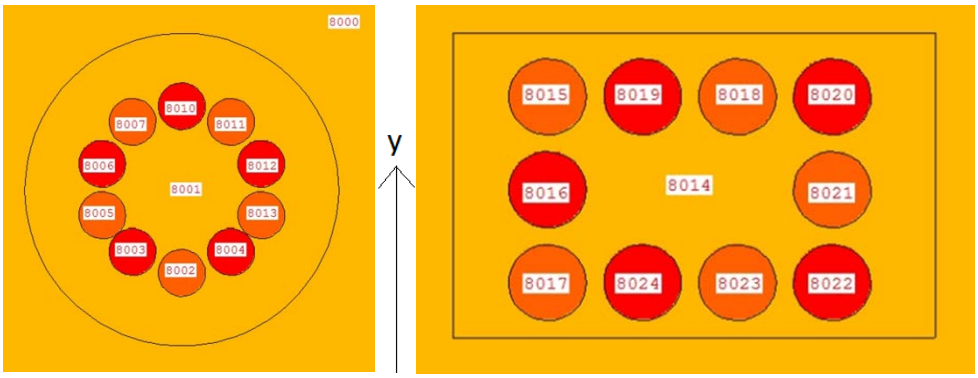

Figure 11. Circular (left) and Rectangular (right) holder for configuration inside moderator The neutron source (FNG target) is in front of holders 8002, and 8023-8024.

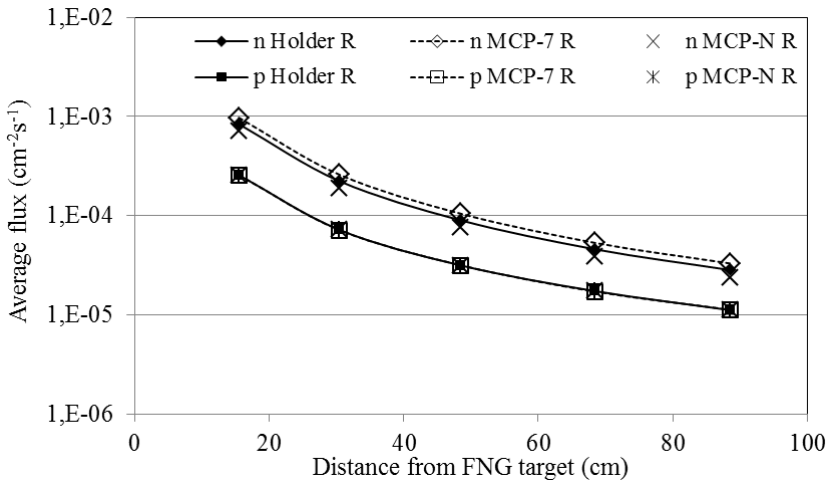

Figure 12. Average neutron (n) and gamma (p) fluxes over MCP-7 and MCP-N and overall TLDs in rectangular holders (1/cm^2/source). Irradiation inside moderators under DD.

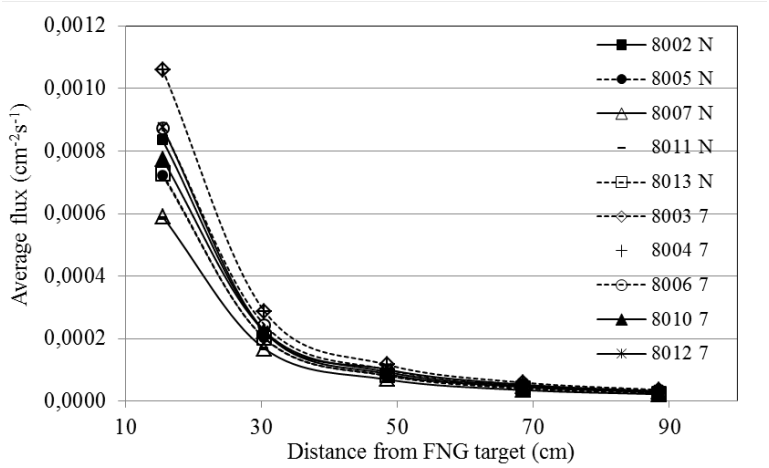

Figure 13. Neutron flux per source neutron in individual TLDs inside circular holder at various distance from FNG source in moderator under DD irradiation (cells are in figure 9).

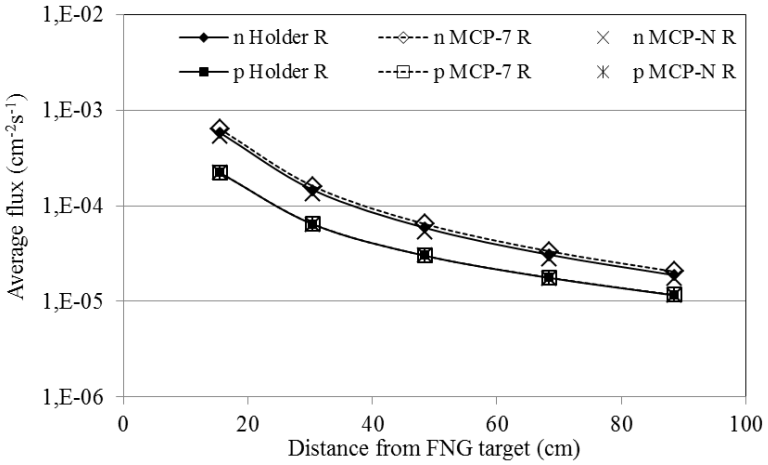

Figure 14. Average neutron (n) and gamma (p) fluxes per source neutron over MCP-7 and MCP-N and overall TLDs in rectangular holders). Irradiation inside moderators under DT.

2.2.2. DD and DT irradiations

Bare samples in rectangular holders and configuration in rectangular and cylindrical holders inside moderators (same assembly as JET experiment) were irradiated under DD neutrons in the week 22-25 November 2016 and under DT neutrons on 6 December 2016, after the replacement of the FNG target. Bare irradiations were performed at 6 radial positions from 5.5 to 88.5 cm as shown in figures 4 and 15. Detectors in rectangular holders have been fixed on a PVC support rail. An indium foil has been located behind the holder in the last position for an independent measurement of the neutron fluence. Bare irradiations lasted about 3 hours under DD and few minutes under DT. The total neutron yield in both irradiations was fixed to ~2.23×10^{12} n and the fluence at detectors positions was estimated by the MCNP calculations reported above for DD and DT irradiations (Table 1). FNG neutron yield was measured through the calibrated surface barrier silicon detector installed close to the FNG target.

Irradiations were also performed inside polyethylene moderators in the same five positions as the “bare” configuration (except for the first one at the 5.5 cm as it was too close for holder in moderator). The isocentre of the FNG beam was directed to the middle of rectangular holders facing the beam. The positions of the experimental set-up are in figure 16. The irradiations lasted between 55 min

and 106 min under DD, and few minutes under DT to provide to the TLDs, inside the moderators, the same levels of fluence as bare. The neutron yield from bare to irradiation in moderator was scaled on the basis of the MCNP calculations. The details of the irradiations under DD and DT are reported in Tables 2 and 3, respectively.

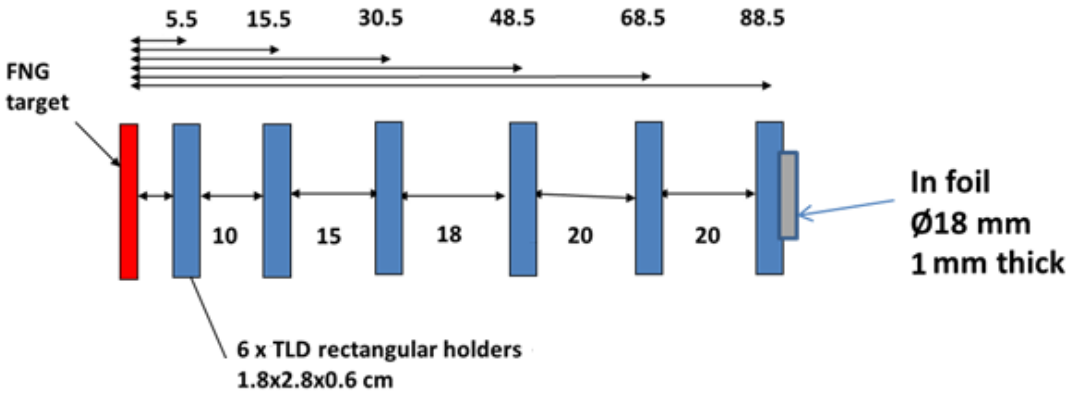

Figure 15. Layout of TLD bare irradiation at FNG.

*Table 1. Neutron fluence at the detectors in bare holders under DD and DT**

Distance from target (cm)	N fluence (n/cm^2)	
	DD	DT
5.5	1.08×10^{10}	5.60×10^{9}
15.5	1.27×10^{9}	6.98×10^{8}
30.5	2.94×10^{8}	1.76×10^{8}
48.5	1.08×10^{8}	6.96×10^{7}
68.5	5.22×10^{7}	3.51×10^{7}
88.5	2.97×10^{7}	2.14×10^{7}

*from MCNP analysis

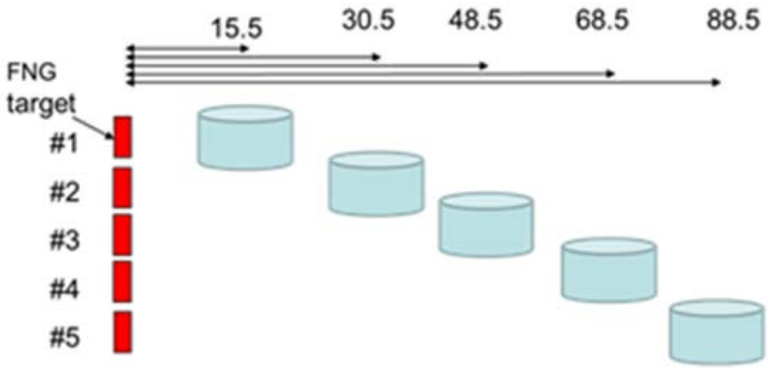

Figure 16. Layout of TLD irradiations in moderators at FNG.

Table 2. Details of irradiation in moderator under DD and estimated neutron fluence at the detectors positions.

Irrad. #	Distance from the target (cm)	Irrad. time (s)	DD yield (n)	Fluence in rectangular holder (n/cm^2)*	Fluence in circular holder (n/cm^2)*
#1	15.5	6374	1.18 x10^{12}	9.92x10^8	9.55x10^8
#2	30.5	4369	1.07x10^{12}	2.39x10^8	2.41x10^8
#3	48.5	3398	9.26x10^{11}	1.31x10^8	1.32x10^8
#4	68.5	3614	8.87x10^{11}	4.07x10^7	4.29x10^7
#5	88.5	3314	8.81x10^{11}	2.51x10^7	2.59x10^7

* from MCNP analysis

Table 3. Details of irradiation in moderator under DT and estimated neutron fluence at the detectors positions.

Irrad. #	distance from the target (cm)	Irrad. time (s)	DT yield (n)	Fluence in rectangular holder (n/cm^2)*	Fluence in circular holder (n/cm^2)*
#1	15.5	306	1.85x10^{12}	1.08x10^9	1.06x10^9
#2	30.5	274	1.72x10^{12}	2.52x10^8	2.53x10^8
#3	48.5	237	1.53x10^{12}	8.98x10^7	9.38x10^7
#4	68.5	221	1.47x10^{12}	4.51x10^7	4.59x10^7
#5	88.5	221	1.49x10^{12}	2.80x10^7	2.87x10^7

* from MCNP analysis

2.3. Irradiations at the thermal neutron facility

Irradiations in thermal neutrons field were carried-out in the thermal neutron facility at INMRI (Istituto Nazionale di Metrologia delle Radiazioni Ionizzanti) laboratories in ENEA Casaccia. The facility consists of a reactor graded graphite cylinder (25 cm diameter, 20 cm high), surrounded by a 13.5 cm thick polyethylene reflector, which acts as moderator and shielding. Six Am-Be neutron sources (individual neutron emission rate of about 10^6 s^{-1}) are located in the polyethylene reflector at angular distances of 60°. The standard was recently calibrated giving a fluence rate of $1.15 \cdot 10^4$ ±1% cm^{-2}s^{-1}, a spatial uniformity of ±0.2% over a volume 4 cm high and 2 cm in diameter and a cadmium ratio equal to 8 ±2%. The facility and the neutron spectra calculated with FLUKA code are shown in figure 17.

Five samples of MCP-N and MCP-7 in circular holders were exposed to thermal neutrons from 30 minutes to 48 hours, providing thermal neutron fluence in the range 2x10^7 -2x10^9 n/cm^2 (Table 4). Pictures of the lay-out of installation of the TLDs are shown in figure 18. The irradiation time and fluences are summarised in Table 4.

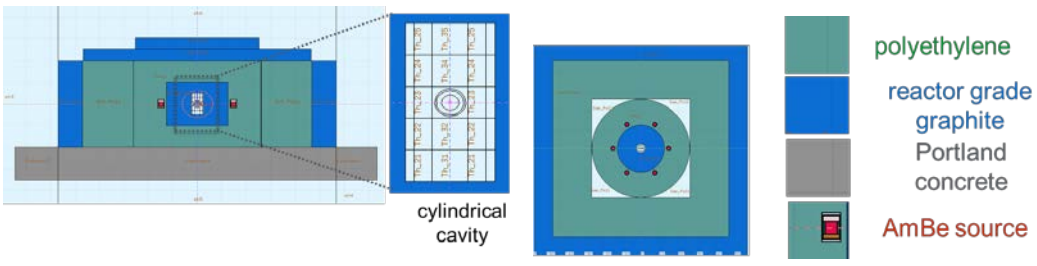

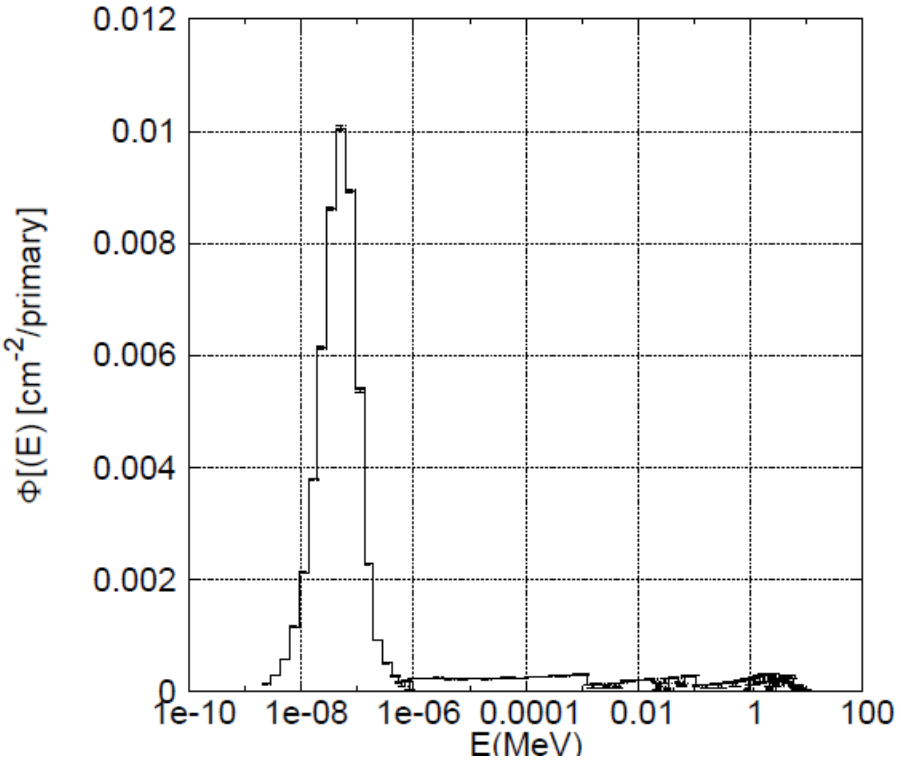

Figure 17. FLUKA model of the thermal neutron facility at INMRI (top) and neutron fluence energy spectrum inside the cavity (bottom).

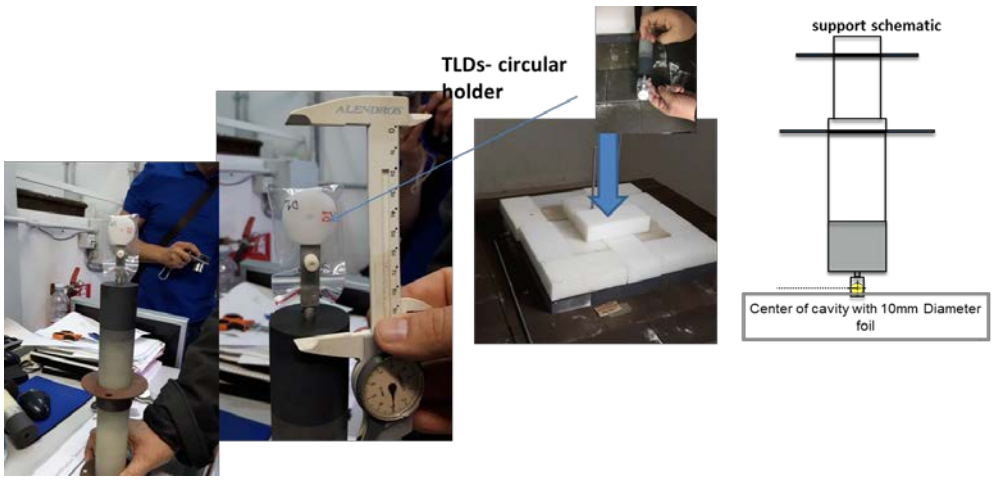

Figure 18. Lay-out of installation of TLDs holder on the plug for irradiation in thermal neutron facility.

Table 4. Exposure time and thermal neutron fluence of TLDs irradiation.

Exposure time (hours)	Thermal fluence (n/cm^2)
0.5	2.1x10^7
2	8.3x10^7
4	1.7x10^8
18	7.5x10^8
48	2.0x10^9

2.4. Irradiations under Co-60 gamma radiation

Irradiations with Co-60 gamma radiation at ENEA INMRI irradiation facility currently used for calibration of radiotherapy dosimeters were performed on 23 November to complement the gamma calibration with Cs-137 carried-out in Poland. TLD samples of MCP-N & MCP-7 in proper circular holder were exposed at Co-60 source to air kerma of 100 mGy, 1 Gy and 5 Gy. The dose range was selected to be relevant for JET application and below saturation at high doses. The TLDs irradiations were carried out at a distance from the source of 100 cm with a beam size of 10 cm x10 cm and air kerma rate of 2.84 mGy s^{-1}. The beam uniformity across the samples was within 0.2%. The samples were irradiated free in air with a build-up material realizing the electronic equilibrium conditions.

2.5. TLDs' readout process and elaboration of experimental results.

After the experimental campaigns, the TLDs were transported back to IFJ Kraków. Here they have been unpacked from the PE containers/boxes and prepared for the readout process. The calibration TLDs (remained at the IFJ) have been divided in two parts and irradiated with gamma rays to provide 10 mGy Cs-137 air kerma at the Secondary Standard Calibration Laboratory of the IFJ (detectors were irradiated in the PMMA box providing proper secondary electron equilibrium condition).

The readout campaign started on 12 December 2016 and ended on 9 January 2017. Readout has been done using Harshaw 3500 manual TL reader. All detectors together with the calibration detectors have been annealed at 100°C for 10 min. before readout, then readout in nitrogen atmosphere (140 l/h flow) with rate 2°C/s in the temperature range 100-270°C.

3. Experimental results

3.1. Results of DD, DT and thermal neutron exposures derived in γ-ray calibrated air kerma

The TL signal measured for all detectors have been calibrated in terms of air kerma with Cs-137 gamma rays. For gamma rays, it can be demonstrated that air kerma is equivalent to dose in air under the charged particle equilibrium conditions provided by the PE boxes. Results of measurements taken at the different positions are derived as the mean value of the signals of MCP detectors' of the same type (five detectors at each position) The standard uncertainty of measurements given with the values includes not only the uncertainty of detectors readout but also the uncertainty of the Cs-137 gamma calibration.

3.2. Results of Co-60 exposures

The results after background subtraction for air kerma for MCP-7 and MCP-N detectors irradiated by Co-60 gamma are shown in Table 5. Good accuracy of gamma measurements was achieved taking into account the combined standard uncertainty of irradiation (0.7%). The difference in efficiency of MCPs' detection of gammas with Co-60 (exposure source) and Cs-137 (calibration source) energy which is close to 10% for bare detectors (see e.g.: [19, 20]). This is well established in the literature of the subject that MCPs' efficiency of gammas for Co-60 energy is higher than for Cs-137 gammas' energy, while for MTSs' the difference is opposite. The differences in doses absorbed by MCP-N and MCP-7 are very small taking into account the uncertainty of the measurements. The same situation is observed for all background dosemeters. The background and transport dose registered is at the level of 0.1 mGy during the whole period between annealing and readout of the dosemeters.

Table 5. MCP-7 and MCP-N detectors' Co-60 gamma results derived as mean value of the same type detectors' response calibrated in air kerma with Cs-137 gamma rays.

Co-60 exposure value (mGy)	MCP-7		MCP-N	
	Average K_a (mGy)	K_a uncertainty (mGy)	Average K_a (mGy)	K_a uncertainty (mGy)
100	95.700	1.599	97.024	1.912
1000	965.094	17.343	970.445	19.078
5000	5044.783	78.471	5043.749	100.408

3.3. Results from neutron irradiations

LiF detectors are sensitive to neutrons, their response to neutrons being enhanced by ^{6}Li-enriched lithium or almost suppressed by using lithium consisting entirely of ^{7}Li. In general, the response of the TLDs can be expressed as follows:

$$R_{tot}(7,N)_{MCP} = R_{\gamma} + R_n(7,N)_{MCP} \quad (1)$$

where R_{tot} is total response of detector of each type (MCP-N or MCP-7), R_{γ} is its response to non-neutron part of the radiation field (in our case at JET mostly gamma radiation), while R_n is its response to thermal neutrons. These quantities are calibrated with gamma rays in terms of air kerma:

$$K_a(7,N) = K_{\gamma} + K_n(7,N) \quad (2)$$

where K_{γ} is the air kerma (gamma dose) due to ɣ-rays and K_n is air kerma due to neutrons. K_a represent the net air kerma from which the background has been already subtracted. The part of the registered signal which is due to neutron component of the field when calibrated with gamma rays depends not only on the type (7, N) and material (MCP) but also on geometry of the detector. As MCP-7 detectors contain only about 0.03% of Li-6, it can be assumed in a first approximation that almost all their response is due to non-neutron component of the field of radiation.

$$K_a(7) \approx K_{\gamma} \quad (3)$$

Under this assumption, the difference K_a(MCP-N)-K_a(MCP-7) represents, in a first approximation the contribution due to the neutron component of the field. However, it should be noted that actually MCP-7 are also sensitive to neutron component, though much less than non-neutron (as they contain only about 0.03% of Li-6), and the equation (3) is no longer valid. In the approach followed for JET assessment described below, its response to neutrons is also considered.

The difference K_a(MCP-N)-K_a(MCP-7) derived for thermal neutron exposures' results at each position is given in table 6. The registered background and transport dose is on the level of measurement accuracy (0.001±0.003 mGy) and was subtracted from all values. The same difference derived from measurement for both DD and DT exposures' results at each position are presented at table 7. For both MCP-7 and MCP-N detectors we used the mean value of all detectors response measured at each position together with total uncertainty calculated for each value. The background and transport dose was subtracted (0.004±0.004 mGy for DD and 0.001±0.005 mGy for DT irradiation). K_a(MCP-N)-K_a(MCP-7) values in DT bare conditions are negative or too small, so these data are unreliable.

Table 6. K_a(MCP-N)-Ka(MCP-7) difference for thermal neutron irradiation.

Thermal fluence (n/cm^2)	K_a(MCP-N)-K_a(MCP-7) (mGy)	Total uncertainty (mGy)
$2.0x10^9$	155.829	4.412
$8.3x10^8$	58.413	0.963
$1.7x10^8$	12.604	0.227
$8.3x10^7$	6.308	0.108
$2.1x10^7$	1.544	0.029

Table 7. K_a(MCP-N)-K_a(MCP-7) difference for DD and DT irradiations.

			DD irradiation		DT irradiation	
	Holder	Distance from the FNG target [cm]	K_a(MCP-N)-K_a(MCP-7)		K_a(MCP-N)-K_a(MCP-7)	
			Average values [mGy]	Total uncertainty [mGy]	Average values [mGy]	Total uncertainty [mGy]
Moderator	circular	15.5	64.108	5.038	34.806	1.981
		30.5	17.025	0.969	8.790	0.369
		48.5	9.255	0.561	3.206	0.125
		68.5	2.721	0.139	1.525	0.065
		88.5	1.733	0.088	0.964	0.040
	rectangular	15.5	63.212	0.816	35.647	1.002
		30.5	16.438	0.187	8.567	0.250
		48.5	8.967	0.127	3.134	0.096
		68.5	2.595	0.044	1.504	0.046
		88.5	1.676	0.021	0.932	0.031
Bare		5.5	0.617	0.231	-1.922	2.647
		15.5	0.130	0.015	-0.210	0.263
		30.5	0.065	0.006	-0.024	0.072
		48.5	0.053	0.005	0.000	0.033
		68.5	0.050	0.005	0.018	0.020
		88.5	0.039	0.005	0.022	0.015

3.4 Calibration in terms of neutron fluence

It is worth noting that, while calibrating TLDs in terms of gamma air kerma is straightforward using calibration gamma sources, it is not so for TL neutron signal and therefore, usually, the response of TLDs due to the neutron components is related to the neutron fluence in a well-defined neutron energy spectrum, which is measurable, using the following definitions (instead of Eq.2):

$$K_a(7) = K_\gamma + \alpha_7 \Phi_n \qquad (4)$$

$$K_a(N) = K_\gamma + \alpha_N \Phi_n \qquad (5)$$

where Φ_n is the neutron fluence and $\alpha_{N,7}$ are coefficients (specific also for material used). In particular, the part of TLDs response due to neutron component of the radiation field can be related to the local neutron fluence using the LiF detectors' calibration performed in 2006 by Burgkhardt et al. at the PTB Thermal Neutron Reference Field at GeNF [15, 16], see the Table 8. It can be noted that the response of MCP-7 detectors to neutrons is much smaller than for MCP-N detectors' type, although not zero. (α_N-α_7) value according Burgkhardt et al. [16] (see table 8) is 3.97×10^{-8} mGy/(n/cm^2).

Table 8. TLDs and their experimentally determined thermal neutron responses derived by Burgkhardt et al. [16].

Detector	Coefficient	Response to 1 n/cm^2 [mGy]	Standard uncertainty	
			meas. [%]	total [%]
MCP-N	α_N	4.10×10^{-8}	1.5	5.2
MCP-7	α_7	1.30×10^{-9}	1.2	5.1
(MCP-N)-(MCP-7)	α_N- α_7	3.97×10^{-8}	1.6	5.4

In the case of JET measurements, although the neutron spectrum is not thermal in the Torus Hall, the large PE moderators are used to ensure that the enclosed TLDs "see" a pure thermal neutron field. With this assumption the 'Burgkhardt' coefficients have been used at JET for evaluating the neutron fluence from TLD measurements up to now [1-5]. Actually, the TLDs calibration factors from Burgkhardt are not rigorously correct for detectors located close to the tokamak because the neutron field inside the PE cylinder is not fully thermalized in such positions and the detectors are exposed to a non negligible fast neutrons component. Analyses of the results of the calibration experiments at the ENEA allowed for determination of new calibration factors, i.e. α_N-α_7 coefficients calculated for real fusion environment.

Taking into account evaluated results presented in &3.3 we have calculated the new calibration coefficients 'air kerma to neutron fluence' and the related uncertainty according to formulas presented below.

The Air kerma to neutron fluence coefficients were evaluated using Eqs.4-5. The $\alpha_{N,7}$ coefficients were first obtained from Eqs.4-5 as angular coefficients of the straight lines of $K_a(N)$ and $K_a(7)$ versus the total fluence Φ_n. The results are given in Table 9.

Table 9. Average α_N and α_7 coefficients for the MCP-N and MCP-7 detectors system in different neutron energy spectra.

	Thermal	DD mod	DT mod	DD bare	DT bare
α_N	8.22×10^{-8}	7.09×10^{-8}	3.89×10^{-8}	5.44×10^{-10}	1.07×10^{-8}
α_7	4.53×10^{-9}	2.99×10^{-9}	4.91×10^{-9}	4.67×10^{-10}	1.11×10^{-8}
$\alpha_N - \alpha_7$ (*)	7.77×10^{-8}	6.79×10^{-8}	3.40×10^{-8}	7.63×10^{-11}	-3.85×10^{-10}
Error on average $\alpha_N - \alpha_7$	2.49×10^{-9}	1.74×10^{-9}	1.02×10^{-9}	5.48×10^{-11}	6.31×10^{-10}
% error on average $\alpha_N - \alpha_7$	3.21%	2.56%	3.01%	71.76%	164.15%

(*) difference obtained from α_N and α_7 evaluated separately

The method provides also the $K\gamma$ values as intercepts on the y axis which, however, are not very accurate due to the fact that the gamma contribution is very small. As a consequence, the use of Eq.(4) and Eq.(5) separately, i.e. the use of only MCP-N or MCP-7 to determine the neutron fluence can be affected by the uncertainty on $K\gamma$. The combined use of both MCP-N and MCP-7 can be more accurate by using Eq.(6).

$$\alpha_N - \alpha_7 = \frac{[K_a(N) - K_\gamma] - [K_a(7) - K_\gamma]}{\Phi_n} = \frac{K_a(N) - K_a(7)}{\Phi_n} \qquad (6)$$

The calculated values of α_N-α_7 coefficients from Eq.6 for all measurements in all performed experiments are presented in Figure 19. The coefficients show a flat fluence response in all experiments and the variability of the values are caused by the differences in the applied neutron energy spectra. Due to the large spread of results (over one order of magnitude), for bare irradiation an additional scale on the axis on the right side of the graph was used. The total uncertainty in α_N-α_7 is obtained by considering the standard deviations of $K_a(N)$ and $K_a(7)$, and the standard deviation of neutron fluence assumed to be ±10% for DD experiment, ±4-6% for bare irradiation under DT, ±4% for DT experiment in moderators and ±5% in thermal neutron field.

The difference of about a factor 2 between α_N, α_7 and α_N-α_7 coefficients obtained in thermal field in this work and 'Burgkhardt' factors can be explained by the irradiation geometry. The GeNF thermal neutron radiation field was a plane parallel beam; the 'Burgkhardt' coefficients were evaluated as mean value of results for three applied neutron fluences. In contrast, here we have applied thermal neutron field isotropically in the volume of irradiation chamber. In this approach we have exposed the entire surface of the detectors with thermal neutrons whilst at GeNF experiment only one side of detector absorbed neutrons.

The average values α_N-α_7 of with related uncertainty are given in table 10. These values represent the calibration coefficients for the MCP-N and MCP-7 TLDs system to measure the neutron fluence in different neutron energy spectra. K_a(MCP-N)-K_a(MCP-7) values in DT bare conditions are negative or too small (see table 7), so these data are unreliable. DT fast neutrons are not registered by the MCP-N detectors without a moderation hence the signals for MCP-N and MCP-7 are comparable for DT. Note that the α_N-α_7 coefficients obtained from Eq.6 and given in table 10 differ from those obtained from Eq.4 and 5 and given in table 9 by less than 1.5% for thermal neutron and DT/ DD irradiations in moderators.

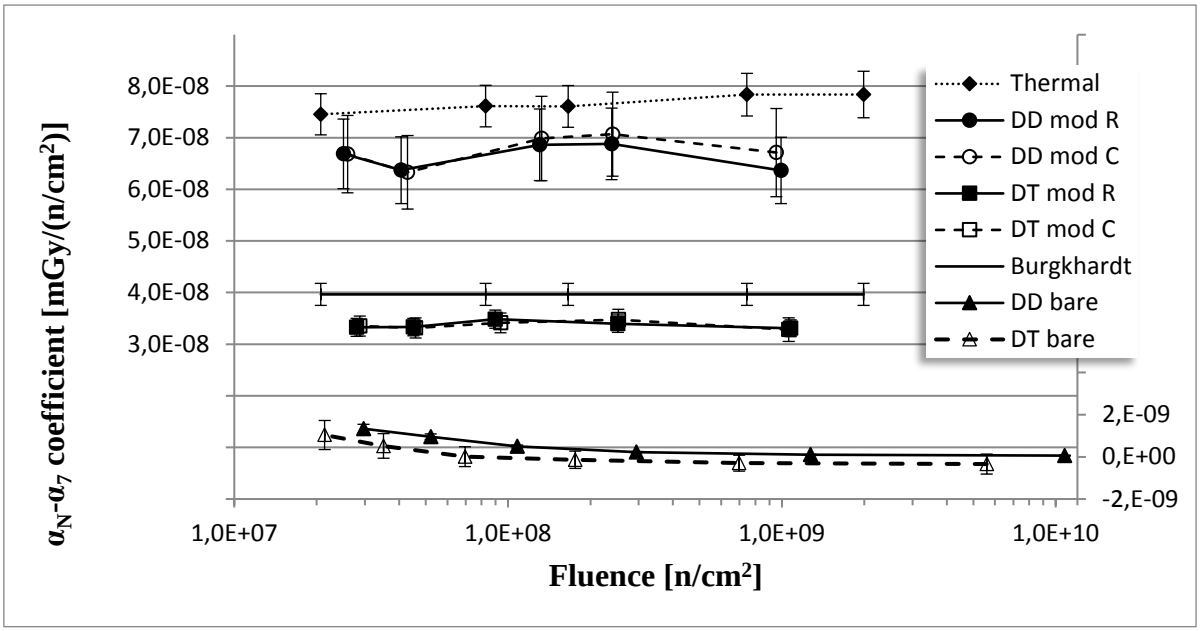

Figure 19. α_N-α_7 coefficients (air kerma to neutron fluence) evaluated from the difference of responses of MCP-N and MCP-7 detectors' types for different neutron spectra in comparison with Burgkhardt et al. [16] calibration factors.

In order to see whether the results could be generalized to any type of spectrum, $(\alpha_N-\alpha_7)^{-1}$ has been plotted against the fraction of low energy component (i.e. E<1 eV) of the neutron spectrum in the conditions of the carried-out calibration campaign. Figure 20 shows the inverse of the average $\alpha_N-\alpha_7$ values versus the percentage of neutrons with energy below 1 eV derived through the spectra calculated with MCNP: the observed correlation indicates that the TLDs assembly can be related to the fraction of thermal neutrons. For the specific MCP-N and MCP-7 system, the calibration curve is $1.59\text{x}10^{9}\ \Phi_n(E<1eV)^{-1.06}$.

Table 10. Average αN-α7 coefficients obtained from the difference of responses of MCP-N and MCP-7 detector system in different neutron energy spectra

	Thermal	DD mod	DT mod	DD bare	DT bare
Average $\alpha_N-\alpha_7$	$7.67\text{x}10^{-8}$	$6.70\text{x}10^{-8}$	$3.37\text{x}10^{-8}$	$5.25\text{x}10^{-10}$	$1.29\text{x}10^{-10}$
Error on average $\alpha_N-\alpha_7$	$4.14\text{x}10^{-9}$	$7.33\text{x}10^{-9}$	$1.87\text{x}10^{-9}$	$1.07\text{x}10^{-10}$	$5.12\text{x}10^{-10}$
% error on average $\alpha_N-\alpha_7$	5%	11%	6%	20%	398%

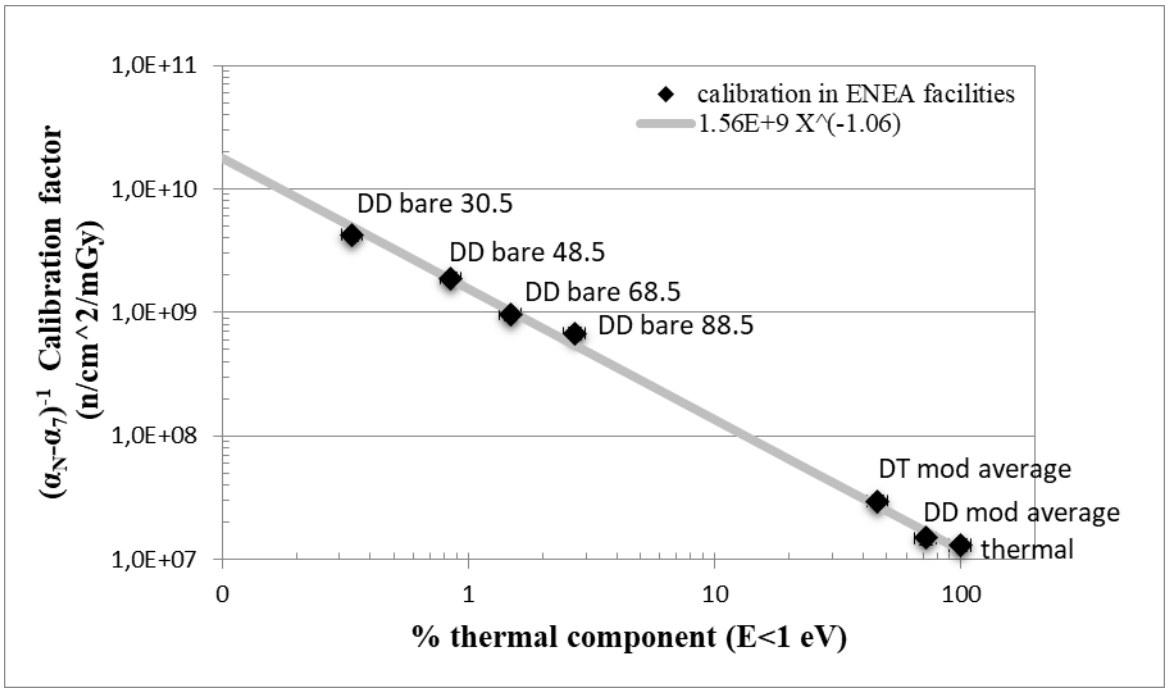

Figure 20. $(\alpha_N-\alpha_7)^{-1}$ versus the % of thermal neutron component in the calibration campaigns at the ENEA facilities. The obtained values can be fitted with a power function.

4. Summary

A neutron fluence measurement system based on the use of MCP-N (^{nat}LiF:Mg,Cu,P) and MCP-7 (^{7}LiF:Mg,Cu,P) TLDs, used at JET to measure low level neutron fluence, have been calibrated in different neutron and gamma fields. The results of the calibration experiments were analysed and the new calibration factors were derived with the related uncertainties. The new coefficients show a flat fluence response in all experiments and the variability of the values are caused by the differences in the applied neutron energy spectra.

The calibration obtained in this work in a thermal neutron field is about a factor 2 higher than that obtained by Burgkhardt in 2006. The difference can be explained by the different irradiation geometry adopted in this work (isotropic neutron field) as compared to that adopted by Burgkhardt (plane parallel neutron beam).

In DD and DT neutron fields the PE moderators do not provide complete moderation of neutrons and the TLDs still “see” fast neutrons. However, it has been found that the calibration factors can be expressed as a function of the fraction of thermal neutron fluence at the position of TL dosemeters in the moderators’ centre. Therefore, the measuring system can be applied to neutron fluence measurements in generic fast neutron fields provided that information on the energy neutron spectrum can be obtained, for instance by simulations. To this end, we will conduct further calibration campaigns at other neutron facilities.

The new calibration factors will be applied to the past and to future JET measurements and will reduce the discrepancies between calculations and measurements observed in past neutron streaming experiment [1-6].

Acknowledgments

This work has been carried out within the framework of the EUROfusion Consortium and has received funding from the EURATOM research and training programme 2014-2018 under grant agreement No 633053. The views and opinions expressed herein do not necessarily reflect those of the European Commission.

References

1. Obryk, B., Batistoni, P., Conroy, S., Syme, B.D., Popovichev, S., Stamatelatos, I.E., Vasilopoulou, T., Bilski, P. and JET contributors, 2014. Thermoluminescence measurements of neutron streaming through JET Torus Hall ducts, Fusion Engineering and Design 89 (9–10), 2235-2240.
2. Batistoni, P., Conroy, S., Lilley, S., Naish, J., Obryk, B., Popovichev, S., Stamatelatos, I.E., Syme, B.D., Vasilopoulou, T. and JET contributors, 2015. Benchmark experiments on neutron streaming through JET Torus Hall penetrations, Nuclear Fusion 55, 053028 (14pp).
3. Vasilopoulou, T., Stamatelatos, I.E., Batistoni, P., Conroy, S., Obryk, B., Popovichev, S., Syme, B.D. and JET contributors, 2015. Neutron streaming along ducts and labyrinths at the JET biological shielding: Effect of concrete composition, Radiation Physics and Chemistry 116, 359–364.
4. Stamatelatos, I.E., Vasilopoulou, T., Batistoni, P., Obryk, B., Popovichev, S., Naish, J. and JET contributors, 2017. Neutron streaming studies along JET shielding penetrations, Proc. of ICRS 13- RPSD 2016, Paris, France, EPJ Web of Conferences 153, 07028 (2017), doi: 10.1051/epjconf/201715307028
5. Villari, R., Batistoni, P., Catalan, J.P., Colling, B., Croft, D., Fischer, U., Flammini, D., Fonnesu, N., Jones, L., Klix, A., Kos, B., Kłosowski, M., Kodeli, I., Loreti, S., Moro, F., Naish, J., Obryk, B., Packer, L., Pereslavtsev, P., Pilotti, R., Popovichev, S., Sauvan, P., Stamatelatos, I.E., Vasilopoulou, T. and JET Contributors, 2017. ITER oriented neutronics benchmark experiments on neutron streaming and shutdown dose rate at JET, Fusion Engineering and Design 107, 171-176.
6. Batistoni, P., Villari, R., Obryk, B., Packer, L.W., Stamatelatos, I.E., Popovichev, S., Colangeli, A., Colling, B., Fonnesu, N., Loreti, S., Klix, A., Kłosowski, M., Malik, K., Naish, J., Pillon, M., Vasilopoulou, T., De Felice, P., Pimpinella, M., Quintieri, L. and JET contributors, Overview of neutron measurements in JET Fusion device, 2018. Radiat. Prot. Dosim., doi: 10.1093/rpd/ncx174
7. Nakajima, T., Maruyama, Y., Matsuzawa, T., Koyano, A., 1978. Development of a new highly sensitive LiF thermoluminescence dosemeter and its applications. Nucl. Instr. Meth. 157, 155-162.
8. Bos, A.J.J., 2001. High sensitivity thermoluminescence dosimetry. Nucl. Instr. Meth. B. 184, 3-28.
9. Obryk, B., Bilski, P., Budzanowski, M., Fuerstner, M., Glaser, M., Ilgner, C., Olko, P., Pajor, A., Stuglik, Z., 2009. Development of a method for passive measurement of radiation doses at ultra-high dose range. IEEE Trans. Nucl. Sci. 56, 3759-3763.
10. Obryk B., Bilski P., Olko P., 2011a. Method of thermoluminescent measurement of radiation doses from micrograys up to a megagray with a single LiF:Mg,Cu,P detector, Radiat. Prot. Dosim, 144, 543–547.
11. Obryk, B., 2013. From nGy to MGy - new dosimetry with LiF:Mg,Cu,P thermoluminescence detectors. AIP Conf. Proc. 1529, 22-29.

12. McKeever, S.W.S., Moscovitch, M., Townsend, P.D., 1995. Thermoluminescence Dosimetry Materials: Properties and Uses. Nuclear Technology Publishing.
13. Obryk, B., Bilski, P., Budzanowski, M., Fuerstner, M., Ilgner, C., Jacquenod, F., Olko, P., Puchalska, M., Vincke, H., 2008a. The response of different types of TL lithium fluoride detectors to high-energy mixed radiation fields. Radiat. Meas. 43, 1144-1148.
14. Obryk, B., Glaser, M., Mandic, I., Bilski, P., Olko, P., Sas-Bieniarz, A., 2011b. Response of various types of lithium fluoride MCP detectors to high and ultra-high thermal neutron doses. Radiat. Meas. 46, 1882-1885.
15. Boettger, R., Friedrich, H., Janßen, H., 2004. The PTB Thermal Neutron Reference Field at GeNF, PTB-N-47, ISBN 3-86509-199-7, http://www.iaea.org/inis/collection/NCLCollectionStore/_Public/36/003/36003698.pdf
16. Burgkhardt, B., Bilski, P., Budzanowski, M., Boettger, R., Eberhardt, K., Hampel, G., Olko, P. and Straubing, A., 2006. Application of different TL detectors for the photon Dosimetry in mixed radiation fields used for BNCT, Radiat. Prot. Dosim. 120, 83-86.
17. M. Martone, M. Angelone, M. Pillon, The 14 MeV Frascati neutron generator, Journal of Nuclear Materials, Volume 212, 1994, Pages 1661-1664.
18. X5 MONTE CARLO Team, MCNP—a general Monte Carlo N-Particle transportcode: version5 user's guide, LANL report LA-CP-03-0245 (2005).
19. Obryk, B., Cywicka-Jakiel, T., Budzanowski, M., Bilski, P., Hranitzky, C., Olko, P., Stadtmann, H., 2008b. Measurements and Monte Carlo simulations of the response of the RADOS personal dosemeters with MTS-N (LiF:Mg,Ti) and MCP-N (LiF:Mg,Cu,P) thermoluminescent detectors to X- and gamma-rays. Radiat. Meas. 43, 616-620.
20. Obryk, B., Hranitzky, C., Stadtmann, H., Budzanowski, M., Olko, P. 2011c. Energy response of different types of Rados personal dosemeters with MTS-N (LiF:Mg,Ti) and MCP-N (LiF:Mg,Cu,P) TL detectors, Radiat. Prot. Dosim. 144, 211-214.